



Optically trapped and controlled microapertures for studies of spatial coherence in an arbitrary light field

W. M. Lee and K. Dholakia

Citation: [Applied Physics Letters](#) **90**, 261101 (2007); doi: 10.1063/1.2751590

View online: <http://dx.doi.org/10.1063/1.2751590>

View Table of Contents: <http://scitation.aip.org/content/aip/journal/apl/90/26?ver=pdfcov>

Published by the [AIP Publishing](#)

Articles you may be interested in

[Optical forces from partially coherent light: Near field of statistically homogeneous sources](#)

AIP Conf. Proc. **1475**, 38 (2012); 10.1063/1.4750088

[Atomic clock based on transient coherent population trapping](#)

Appl. Phys. Lett. **94**, 151108 (2009); 10.1063/1.3120278

[Coherent trapping of x-ray photons in crystal cavities in the picosecond regime](#)

Appl. Phys. Lett. **93**, 141105 (2008); 10.1063/1.2996275

[Continuous light-shift correction in modulated coherent population trapping clocks](#)

Appl. Phys. Lett. **89**, 151124 (2006); 10.1063/1.2360921

[Determination of the Wigner function of an optical field using the atomic Talbot effect](#)

AIP Conf. Proc. **461**, 243 (1999); 10.1063/1.57892

The image shows the cover of an Applied Physics Reviews journal. It features a blue background with a molecular structure. The AIP logo and 'Applied Physics Reviews' text are in the top left. The main title 'NEW Special Topic Sections' is in large white letters. Below it, 'NOW ONLINE' is in yellow, followed by 'Lithium Niobate Properties and Applications: Reviews of Emerging Trends' in white. The AIP logo and 'Applied Physics Reviews' text are in the bottom right.

NEW Special Topic Sections

NOW ONLINE
Lithium Niobate Properties and Applications:
Reviews of Emerging Trends

AIP Applied Physics Reviews

Optically trapped and controlled microapertures for studies of spatial coherence in an arbitrary light field

W. M. Lee^{a)} and K. Dholakia

SUPA, School of Physics and Astronomy, University of St. Andrews, North Haugh, St. Andrews KY16 9SS, United Kingdom

(Received 13 March 2007; accepted 2 June 2007; published online 25 June 2007)

By controlling the rotation rate of a trapped birefringent particle with an optically applied torque, the authors introduce a miniscule wave front deformation at a specific location within an arbitrary light field, with the particle acting as an optical microdiffuser. A trapped birefringent particle and a trapped silica microsphere are positioned to form Young's double slit experiment within a probe light field. The far-field interference from the diffracted optical fields from these particles enable the authors to infer the relative spatial coherence between these local sampling points. With multiple trapped particles, one may perform multipoint coherence analysis of a light field. © 2007 American Institute of Physics. [DOI: 10.1063/1.2751590]

The spatial coherence of a light field^{1,2} is important in numerous areas of both classical and quantum optical science. It dictates the fundamental properties of any propagating light fields such as their directionality and polarization. Spatial coherence of a light field can be modulated through the different Young slit arrangements.^{1,3,4} It is primarily a study of the mutual coherence or phase correlations between a pair of sampling apertures.^{1,2} In a recent study, the traveling surface plasmons between two metallic nanoslits have been shown to modulate the spatial coherence of the light.⁴ Recent studies on supercontinuum light fields^{5,6} have opened up an exciting area in beam shaping of a light field with broad spectral bandwidth. Studying the local spatial coherence of these supercontinuum light fields is of importance for areas such as quantum optical communication,⁷ coherence imaging,⁸ and vortex beam propagation in the presence of atmospheric turbulence.⁹

The spatial coherence of an arbitrary light beam can vary with the different diffracting properties of the sampling apertures. An active control over the location and the induced phase fluctuations of very small (micrometer to nanometer) apertures would effectively allow one to vary the spatial coherence of the light field at different local positions. A rotating diffuser is known to impart random phase fluctuations, over a given time of observation, upon an arbitrary light field with increasing rotation rates of the diffuser.² Hence, if we were able to control the rotation rates of a "microdiffuser" and use that as one aperture within a Young slit-type experiment, we may then actively control and measure the local spatial coherence or phase correlations within an arbitrary optical beam at will.

In this letter, we realize such a microdiffuser through the controlled trapping and rotation of a birefringent microparticle (calcite) held in an optical trap. By varying the rotation rates of our trapped calcite particle, a varying wave front deformation (fine and random phase fluctuations) is controllably introduced upon a localized region of an arbitrary beam. A calcite particle is akin to a diffuser but on a micron scale and possesses minuscule granular surface that deforms the wave front of the incoming light field.² Previously optically trapped spheres, acting as diffracting apertures, have

been used to probe a vortex trapping beam.¹⁰ By contrast, here we use a dual beam optical trapping system¹¹ to independently control the positions of each of the optical apertures within a second (arbitrary) optical light field. This setup decouples the control of the apertures from the investigated light field of interest.¹⁰ Optical forces and torques¹² from the traps allow us to remotely control both the position and the rate of rotation of the microdiffuser at any part of the light field. The rotation is imposed by using a circularly polarized trapping field that imparts spin angular momentum to our trapped (birefringent) object. By varying the optical power of the trapping beam we alter the imparted torque and control the rotation rate of the birefringent particle.¹³ In turn, this alters its diffusing properties upon a localized section of the probed light field. Using a second trapped silica microsphere, as a clear aperture, a Young slit-type experiment is performed upon the probe light field. The relative spatial coherence between the rotating microdiffuser (random phase) and the microaperture (fixed phase) are then measured. With increasing rates of rotation of the microdiffuser, a modulation in the fringe visibility of far-field interference fringes would be expected. In our numerical simulation, we introduce a random phase mask¹⁴ over the aperture E_1 , to simulate the random phase fluctuation introduced by a rotating microdiffuser. Experimentally, the granularity of a single spinning calcite imposes a different phase value over a small area in the sampling beam. With increasing rotation rate, over a given frame of time, the different phase values imparted by the spinning calcite would appear random and thus spatially incoherent with the rest of the sampling beam. Numerically, we provide a simple approximation where a random phase mask creates a range of phase values distributed over one of the apertures to simulate the effects of the rotating calcite. With higher phase variation that is distributed over the phase mask, the phase from the selected aperture would become more spatially incoherent with respect to the rest of the sampling beam.

We numerically analyze the far-field interference pattern from a randomized aperture E_1 and a clear aperture E_2 placed in a coherent light field, i.e., an annular Laguerre-Gaussian (LG) beam with azimuthal index $l=3$ and radial index $p=0$, as illustrated in Fig 1(a). LG beams have been of interest for a wide range of studies in recent years^{7,9,10,15} and here take

^{a)}Electronic mail: wml6@st-andrews.ac.uk

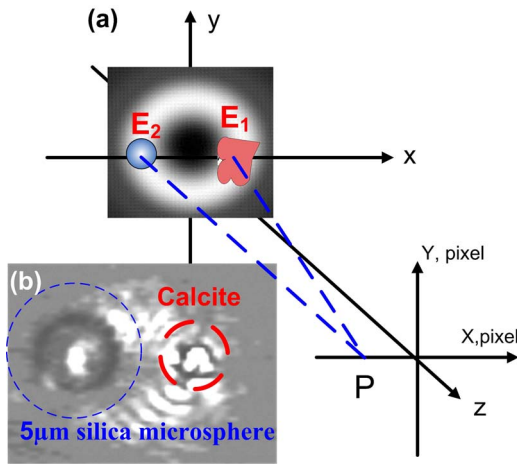


FIG. 1. (Color online) Placement of two apertures around the annular ring of the LG ($l=3$, $p=0$) beam. (a) is a schematic of the experiment. The irregular aperture (E_1) illustrates the microdiffuser and the circle (E_2) denotes a smooth microsphere. The irradiating light fields from the two apertures, E_1 and E_2 , interfere in the far field and P denotes the observation point in the far field. (b) shows an experimental image of a calcite particle (encircled with a thick dashed line) trapped simultaneously with a $5\ \mu\text{m}$ diameter silica sphere (encircled with a thin dashed line) placed within the annular intensity ring of the LG beam.

the role of the arbitrary coherent light field in our experiment. A randomized aperture E_1 is generated by multiplying the complex amplitude of the diffracting disk with a randomized phase function given by $e^{-i\text{rand}[\alpha, \beta]}$, where $\text{rand}[\alpha, \beta]$ is a random phase generator and α, β are the lower and upper limit of the phase variation (α is set at zero and β is left to vary). The random phase aperture E_1 aims to simulate the random phase fluctuation introduced by a rotating microdiffuser, which is a microscopic calcite particle, as shown in Fig. 1(b). The output fields from the apertures, E_1 and E_2 , are then propagated numerically towards the far field P using split-step Fourier method.¹⁰ These two apertures create a Young slit interference that samples the wave front of the LG beam at two specific points over a given time,¹⁰ where the visibility $V(r)$ of the interference fringes indicates their degree of spatial coherence. The visibility $V(r)$ of the interference fringes in the far field is the division of the difference and sum of the maximum $I_{\max}(r)$ and minimum $I_{\min}(r)$ of the intensity of the fringes on point P at position r , where $r = \sqrt{x^2 + y^2}$, as shown in Fig. 1 and $|\gamma_{12}|$ is the modulus of the mutual complex coherence between the optical field emerging from two apertures (E_1 and E_2 , as seen in Fig. 1) at a given time, thus ignoring the effects from temporal coherence.

$$V(r) = \frac{I_{\max}(r) - I_{\min}(r)}{I_{\max}(r) + I_{\min}(r)} = |\gamma_{12}|. \quad (1)$$

The significance of Eq. (1) is that the visibility $V(r)$ of the interference pattern in the far field is directly related to the correlation of the phase fluctuation between the two apertures E_1 and E_2 .¹ The local visibility $V(r)$ is also equal to the modulus of complex degree of coherence γ_{12} .

In Fig. 2(a), we show the experimental setup. A dual beam trapping system is formed by two orthogonal polarized beams from a 1070 nm fiber laser (5 W, IPG, Photonics), built around a Nikon TE2000U inverted microscope platform. The two orthogonally linearly polarized beams are formed using two polarizing beam splitters placed in a

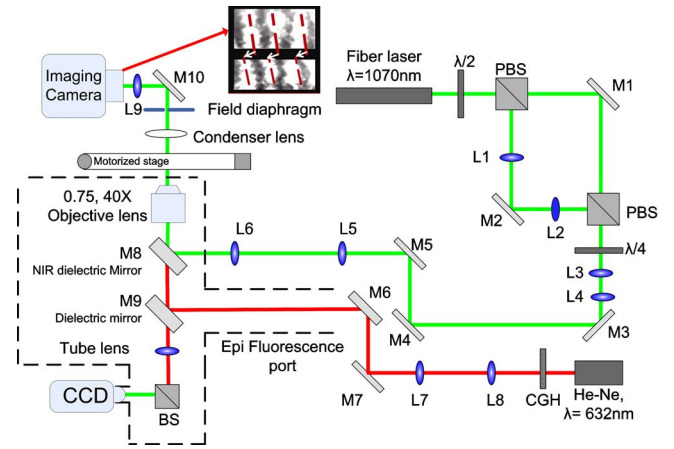


FIG. 2. (Color online) Experimental setup for the two optical traps (Ref. 11) that are formed with orthogonal polarization using a Mach-Zender interferometric-like setup with a half-wave plate and polarizing beam splitters (PBSs). A quarter wave plate is placed to create circularly polarized optical trap. Lenses L1 and L2 form a 1:1 telescope to adjust the axial trapping position of one of the trapping beams. Lenses L3 and L4 form a telescope that expands the trapping beams to fill the back aperture. Lenses L5 and L6 are used to image the steering mirror onto the back focal plane of the objective. A CCD camera (Basler A622f) is placed at the back imaging plane of the condenser assembly. A probe LG beam ($l=3$, $p=0$) is generated using a He-Ne laser beam with a CGH and imaged into the trapping plane using the telescope system (L7 and L8). M1–M5, M8, and M9 denote dielectric mirrors. M6 and M7 denote silver mirrors. [The inset shows the microscopic implementation of the angular Doppler effect (Ref. 16) when the trapped calcite is spun at around 7 Hz, where the interference fringes shift in a periodic manner (denoted by the arrows).]

Mach-Zender interferometer arrangement.¹¹ Both beams then enter a microscope objective (numerical aperture of 0.75, 40 \times) to form two independent optical traps. The sample is a mixture of crushed calcite and $5\ \mu\text{m}$ silica microspheres that are dispersed in a D_2O solution, used to reduce heating effects from laser absorption. We note that the coarseness (granularity)² of the calcite is an important part of reducing the coherence as oppose to the use of a more uniform birefringent particles such as vaterite. The particles are placed in a cylindrical sample chamber of diameter 1 cm and depth 100 μm . A quarter wave plate is then inserted to generate circularly polarized trapping beams. One of the beams traps and rotates the calcite particle through the transfer spin angular momentum, while the other beam forms a single beam trap to tweeze a $5\ \mu\text{m}$ silica microsphere, as shown in Fig. 1(b). As noted above, the light field which we choose to sample here is a LG beam ($l=3$, $p=0$) generated using a computer generated hologram¹⁵ (CGH) at a wavelength of 632 nm (He-Ne, Spectra Physics, USA) and is simultaneously focused through the same objective as the trapping beams via the epifluorescence port of the microscope. In the far field, we obtain fringes from the light diffracted by microapertures placed within the LG beam using a charge coupled device (CCD) camera operating at a low frame rate. By controlling the rotation rate of the calcite particle in one of the optical traps at around 7 Hz, we obtain reasonably good fringe visibility (measured visibility V of the fringes is around 0.71 ± 0.01). We also observe that the interference fringes start to move laterally in a continuous manner, as shown in the inset of Fig. 2 denoted by the arrow. In this case, the birefringent particle behaves like a rotating aperture, with slight diffusing properties. The fringe motion, as observed, is due to the rotational frequency difference be-

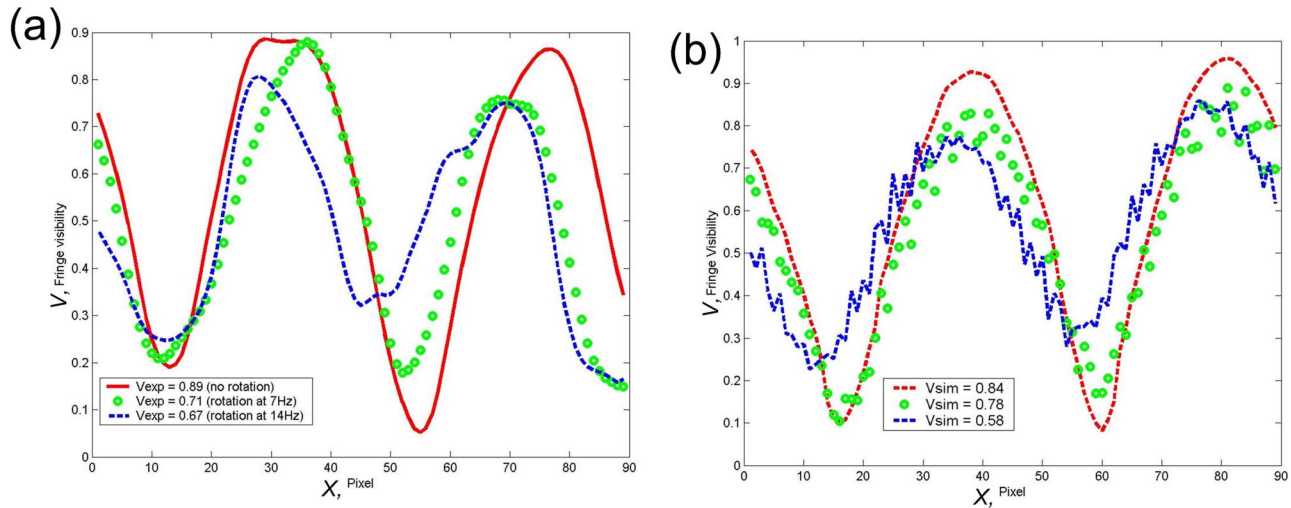


FIG. 3. (Color online) (a) is the experimental data of the interference fringes from two apertures placed around the annular ring of the LG₀₃ beam. (b) shows the numerically calculated far-field interference fringes when one of the apertures possesses a random complex phase. (a) shows that by experimentally increasing the rotation of the calcite particle, we can observe a decrease in the fringe visibility V_{exp} . This is seen numerically as well in V_{sim} , as shown in (b), increasing the phase variation in one of the apertures. (V_{exp} denotes the average fringe visibility obtained experimentally and V_{sim} denotes the average visibility obtained numerically.) The interference fringes are distributed transversely across the X axis, which is measured in pixel size for both (a) and (b).

tween the two apertures, realizing a microscopic version of the angular Doppler effect.¹⁶

Upon closer examination of the experimental data [Fig. 3(a)], we observe that at higher spin rates of the calcite the corresponding far-field interference fringes show a significant decrease in their visibility. From the experimental results in Fig. 3(a), when the trapped calcite is not rotating, the corresponding interference fringes have a measured visibility to be approximately $V_{\text{exp}} = 0.89 \pm 0.01$. However, when the calcite is being spun at a spin rate of around 7 Hz, we observe that the visibility of the interference fringes drops to $V_{\text{exp}} = 0.71 \pm 0.01$. With a further increment of the spin rate of the calcite to approximately 14 Hz, we can see that the visibility drops further to $V_{\text{exp}} = 0.67 \pm 0.01$. We numerically calculate the expected visibility that we might expect from a simulated microdiffuser (random phase) and a second clear aperture (fixed phase) placed in a LG ($l=3$, $p=0$) beam. In Fig. 3(b), a clear decrease in the visibility of the far-field interference fringes is observed by increasing the random phase variation $e^{-i\text{rand}[0,\beta]}$ of E_1 , where $0.32\pi \leq \beta \leq 0.95\pi$. This decreases the phase correlation between the two sampling points E_1 and E_2 .¹⁴ By generating a random phase where $\alpha=0$ and $\beta=0.32\pi$, we observe that the calculated fringe visibility drops to $V_{\text{sim}}=0.84$, denoted by red line. A further increase of the random phase variation β to 0.64π and β to 0.95π , results in the fringe visibility dropping to $V_{\text{sim}}=0.78$ and $V_{\text{sim}}=0.58$, denoted by green circle and the blue dotted line, respectively. From both the experimental results and the numerical results, we can see that the visibility of the interference fringes reduces with increasing phase fluctuations in one of the sampling apertures. By comparing the numerical calculations (V_{sim}) and experimental results (V_{exp}), we can see that a rotating calcite at rates from 7 to 14 Hz can approximately introduce a random phase variation β from 0.64π to 0.95π .

In conclusion, we have demonstrated that the optically controlled rotation of the birefringent microparticle (calcite) imposes fine random phase fluctuations upon a local spatial position within the wave front of a probe light field and thus modulates the relative phase relation (spatial coherence) with

a second sampling point. The reduction in the visibility of the calculated and the experimentally observed far-field interference pattern is seen to be comparable. An optically rotating birefringent particle (calcite) thus fulfils the role of a microdiffuser. Optically trapped microapertures are simple to control and possess a high degree of localization and maneuverability. Future studies could include the study of spectra shift on polychromatic light fields^{5,6} using nanoparticles¹² and multipoint spatial coherence measurements¹⁷ using multiple optically trapped and rotating particles.¹⁸

This work is supported by the European Science Foundation grant NOMSAN which was supported by funds from the UK Engineering and Physical Sciences Research Council and the European Framework 6 Programme. One author (W.M.L.) acknowledges Einst Technology Pte Ltd. for the support and Klaus Metzger for his technical assistance.

¹E. Wolf, Proc. R. Soc. London, Ser. A **225**, 96 (1954).

²W. Martienssen and E. Spiller, Am. J. Phys. **32**, 919 (1964).

³L. D. A. Lundeberg, G. P. Lousberg, D. L. Boiko, and E. Kapon, Appl. Phys. Lett. **90**, 021103 (2007).

⁴C. H. Gan, G. Gbur, and T. D. Visser, Phys. Rev. Lett. **98**, 043908 (2007).

⁵H. I. Sztul, V. Kartazayev, and R. R. Alfano, Opt. Lett. **31**, 2725 (2006).

⁶P. Fischer, C. Brown, J. Morris, C. López-Mariscal, E. Wright, W. Sibbett, and K. Dholakia, Opt. Express **13**, 6657 (2005).

⁷A. Mair, A. Vaziri, G. Weihs, and A. Zeilinger, Nature (London) **412**, 313 (2001).

⁸Z. Ding, H. Ren, Y. Zhao, J. S. Nelson, and Z. Chen, Opt. Lett. **27**, 243 (2002).

⁹C. Paterson, Phys. Rev. Lett. **94**, 153901 (2005).

¹⁰W. M. Lee, V. Garcés-Chávez, and K. Dholakia, Opt. Express **14**, 7436 (2006).

¹¹E. Fallman and O. Axner, Appl. Opt. **36**, 2107 (1997).

¹²K. Dholakia and P. Reece, Nanotoday **1**, 18 (2006).

¹³M. E. Friese, T. A. Nieminen, N. R. Heckenberg, and H. Rubinsztein-Dunlop, Nature (London) **394**, 348 (1998).

¹⁴A. S. Ostrovsky and E. H. García, Rev. Mex. Fis. **51**, 442 (2005).

¹⁵N. R. Heckenberg, R. McDuff, C. P. Smith, and A. G. White, Opt. Lett. **17**, 221 (1992).

¹⁶J. Arlt, M. P. MacDonald, L. Paterson, W. Sibbett, K. Dholakia, and K. Volke-Sepulveda, Opt. Express **10**, 844 (2002).

¹⁷Y. Mejía and A. I. González, Opt. Commun. **273**, 428 (2007).

¹⁸R. L. Eriksen, P. J. Rodrigo, V. R. Daria, and J. Glückstad, Appl. Opt. **42**, 5107 (2003).